

# Arachidonic acid activation of BK<sub>Ca</sub> (Slo1) channels associated to the $\beta_1$ -subunit in human vascular smooth muscle cells

Pedro Martín · Melisa Moncada · Nicolás Enrique · Agustín Asuaje · Juan Manuel Valdez Capuccino · Carlos Gonzalez · Verónica Milesi

Received: 24 October 2013 / Revised: 3 December 2013 / Accepted: 5 December 2013 / Published online: 28 December 2013  
© Springer-Verlag Berlin Heidelberg 2013

**Abstract** Arachidonic acid (AA) is a polyunsaturated fatty acid involved in a complex network of cell signaling. It is well known that this fatty acid can directly modulate several cellular target structures, among them, ion channels. We explored the effects of AA on high conductance Ca<sup>2+</sup>- and voltage-dependent K<sup>+</sup> channel (BK<sub>Ca</sub>) in vascular smooth muscle cells (VSMCs) where the presence of  $\beta_1$ -subunit was functionally demonstrated by lithocholic acid activation. Using patch-clamp technique, we show at the single channel level that 10  $\mu$ M AA increases the open probability (Po) of BK<sub>Ca</sub> channels tenfold, mainly by a reduction of closed dwell times. AA also induces a left-shift in Po versus voltage curves without modifying their steepness. Furthermore, AA accelerates the kinetics of the voltage channel activation by a fourfold reduction in latencies to first channel opening. When AA was tested on BK<sub>Ca</sub> channel expressed in HEK cells with or without the  $\beta_1$ -subunit, activation only occurs in presence of the modulatory subunit. These results contribute to highlight the molecular mechanism of AA-dependent BK<sub>Ca</sub> activation. We conclude that AA itself selectively activates the  $\beta_1$ -associated BK<sub>Ca</sub> channel, destabilizing its closed state probably by interacting with the  $\beta_1$ -subunit, without modifying the channel voltage sensitivity. Since BK<sub>Ca</sub> channels physiologically contribute to regulation of VSMCs contractility and blood pressure, we used the whole-cell configuration to show

that AA is able to activate these channels, inducing significant cell hyperpolarization that can lead to VSMCs relaxation.

**Keywords** PUFAs · Fatty acid · Omega-6 polyunsaturated fatty acid · Human umbilical artery · Patch-clamp · Single channel

## Introduction

Arachidonic Acid (AA), a physiologically relevant 20-carbon omega-6 polyunsaturated fatty acid (PUFA), is an integral component of cell membrane phospholipids, which can be obtained from diet nutrients or synthesized in the liver. In humans, plasma concentration can normally be found in a range of 2.5–13.1  $\mu$ M [8, 41] and could be significantly increased in pathological conditions, such as ischemia [1, 22] and preeclampsia [41]. AA can be released from phospholipids by activation of phospholipase A<sub>2</sub>, and it can then be transformed through different enzymatic pathways mediated by ciclooxigenase, lipooxygenase and cytochrome P450, into a great variety of metabolites (prostacyclins, leucotrienes and epoxyeicosatrienoic acids, respectively) involved in a complex network of cell signaling. These have been implicated in different physiological processes, such as endothelium-dependent blood vessel relaxation, platelet aggregation, stomach mucus and acid secretion, and smooth muscle tone regulation, among others. Moreover, the role of AA metabolites as pro-inflammatory factors has also been demonstrated in several pathological states [9, 13, 36, 38, 42].

Although AA was mainly thought only as a precursor of active metabolites, it is now well-known that AA and other fatty acids (FA) can directly modulate different particular protein structures. Among them, different ion channels (i.e., K<sub>v</sub>, Na<sup>+</sup><sub>v</sub>, Ca<sup>2+</sup><sub>v</sub>, K<sub>2B</sub>, and BK<sub>Ca</sub>) can be inhibited or activated by AA [4, 12, 15, 29, 34] (reviewed by Meves (2008) [32]). In

P. Martín and M. Moncada contributed equally to this work.

P. Martín · M. Moncada · N. Enrique · A. Asuaje · J. M. Valdez Capuccino · V. Milesi (✉)  
GINFIV-CONICET–Grupo de Investigación en Fisiología Vascular,  
Facultad de Ciencias Exactas, Universidad Nacional de La Plata,  
Calles 47 y 115, La Plata 1900, Argentina  
e-mail: veronica@biol.unlp.edu.ar

C. Gonzalez  
CINV–Centro Interdisciplinario de Neurociencia de Valparaíso,  
Facultad de Ciencias, Universidad de Valparaíso, Valparaíso, Chile

particular, the action of PUFAs involving the high conductance  $\text{Ca}^{2+}$ - and voltage-dependent ( $\text{BK}_{\text{Ca}}$ ) channel as the target is emerging as an important non-pharmacological mechanism able to lower blood pressure, since these channels are clearly involved in the physiological regulation of vascular smooth muscle contractility and blood pressure in animals and humans [37]. Furthermore, changes in  $\text{BK}_{\text{Ca}}$  expression or function are associated with human ageing, hypertension, and diabetes [17, 30, 39, 45].  $\text{BK}_{\text{Ca}}$  channels are activated by membrane depolarization and intracellular  $\text{Ca}^{2+}$  concentration. They are tetramers of pore-forming  $\alpha$ -subunits (encoded by *KCNMA1* gene, also named *Slo1*) and can be associated to one of four auxiliary  $\beta$ -subunits codified by *KCNMB1-4* genes. Each one of these confers distinctive functional and pharmacological properties to the resulting  $\alpha$ - $\beta$  channel complex [18, 26, 44]. The differential expression of  $\beta$ -subunits in different cell types could explain the diversity of functions and regulations on the  $\text{BK}_{\text{Ca}}$  channel among diverse tissues and could be used to obtain a tissue-selective  $\text{BK}_{\text{Ca}}$  channel activation, using the auxiliary subunit as a specific molecular target. An example of this is the activation of  $\text{BK}_{\text{Ca}}$  channel by lithocholate, which is only observed in the presence of  $\beta_1$ -subunit [5, 7]. Particularly, in vascular smooth muscle cells (VSMCs),  $\text{BK}_{\text{Ca}}$  channels are highly expressed in association with the  $\beta_1$ -subunit [24, 25]. Recently, Hoshi and colleagues demonstrated that  $\text{BK}_{\text{Ca}}$  channels associated with the auxiliary  $\beta_1$ -subunit are directly activated by docosahexaenoic acid (DHA), a PUFA of omega-3 series and its administration on anesthetized wild-type mice lowers blood pressure. On the other hand, the same treatment has no effect on  $\text{BK}_{\text{Ca}}$  channel knockout mice [21].

In the case of AA, although it is known that it directly activates  $\text{BK}_{\text{Ca}}$  channels [1, 11, 43], the molecular mechanisms of channel activation are not completely understood. Sun et al. have shown in their work with  $\text{BK}_{\text{Ca}}$  expression in *Xenopus laevis* oocytes that AA activates the channel depending on the  $\beta$ -subunit that is present at the time [43]. These authors examined the action of AA on  $\text{BK}_{\text{Ca}}$  channels expressed with or without the  $\beta_2$ -to  $\beta_4$ -subunits, thus finding that it is possible to observe a significant activation of the channel only in the presence of the  $\beta_2$ - or  $\beta_3$ - subunits. Nevertheless, the effects of AA over this channel when found only with  $\beta_1$ -subunit are still unknown.

In the present study, we evaluated the effect of AA on  $\text{BK}_{\text{Ca}}$  channel mediated currents in native human VSMCs where the presence of the  $\beta_1$ -subunit was functionally tested. By using the patch-clamp technique at the single channel level, we observed that this FA induces a significant increase in the open probability of  $\text{BK}_{\text{Ca}}$  channels, mainly by reducing closed dwell time to a great extent. Moreover, we found that AA accelerates the kinetics of voltage channel activation. In whole cell configuration, we demonstrated that AA is able to activate the  $\text{BK}_{\text{Ca}}$  channel and induce significant cell

hyperpolarization in a more physiological context. Finally, by testing the effect of AA on  $\text{BK}_{\text{Ca}}$  channel expressed in HEK293T cells with or without the  $\beta_1$ -subunit, we demonstrated that AA needs the presence of this auxiliary subunit to effectively activate  $\text{BK}_{\text{Ca}}$  channel.

## Methods

### Smooth muscle cell isolation procedure for patch-clamp experiments

Umbilical cords were obtained from normal term pregnancies after vaginal and cesarean deliveries. They were placed in transport solution of the following composition (in millimolars)—130 NaCl, 4.7 KCl, 1.17  $\text{KH}_2\text{PO}_4$ , 1.16  $\text{MgSO}_4$ , 24  $\text{NaCO}_3\text{H}$ , 2.5  $\text{CaCl}_2$ , pH 7.4 at 4 °C and immediately taken to our laboratory where they were stored at 4 °C and used within the next 24 h. All procedures were in accordance with the declaration of Helsinki (1975).

The human umbilical arteries (HUA) were dissected from Wharton's jelly just before the cell isolation procedure. HUA smooth muscle cells (HUASMCs) were obtained by a method based on Klocker's et al. [23] description and later modified in our laboratory in order to diminish the enzyme content in the dissociation medium (DM) [40]. Briefly, a segment of HUA was cleansed of any residual connective tissue, cut in small strips, and placed for 15 min in a DM containing the following (in millimolars)—140 NaCl, 5  $\text{KH}_2\text{PO}_4$ , 5  $\text{MgCl}_2$ , 6 glucose, 5 HEPES; pH was adjusted to 7.4 with NaOH. The strips were then placed in DM with 3 mg/ml collagenase type I during 15–30 min, with gentle agitation, at 35 °C. After the incubation period, the strips were washed with DM, and single HUASMCs were obtained by a gentle dispersion of the treated tissue using a Pasteur pipette. The supernatant, containing our isolated cells, was stored at room temperature (~22 °C) until used. HUASMCs were allowed to settle onto the coverglass bottom of a 3 ml experimental chamber. Only well-relaxed, spindle-shaped smooth muscle cells were used for electrophysiological recordings. Data were collected within 4–6 h after cell isolation.

### Clones and transient transfection

HEK293T cells were grown in Dulbecco's modified Eagle's medium (DMEM) and 10 % fetal bovine serum (FBS) and split when 70–80 % confluent. Human *Slo1*  $\alpha$ -subunit (*KCNMA1*, U11058), the auxiliary subunit  $\beta_1$ -(*KCNMB1*, AF035046), and enhanced green fluorescent protein cDNAs (eGFP) were transiently transfected into HEK cells using FuGene 6. Transfections were done with cDNA encoding for  $\alpha$ -subunits alone or  $\alpha$ + $\beta_1$ -subunit both cloned in pcDNA3 plasmid. The  $\alpha$ + $\beta_1$ -subunit were mixed at 1:3

molar ratios to ensure an excess of  $\beta_1$ -subunit over  $\alpha$ -subunit. When  $\alpha$ -subunits were transfected alone,  $\beta_1$ -cDNA was replaced by empty plasmid. After transfection, cells were kept in culture for 60 h. The electrophysiological measurements were performed 60–70 h after transfection. eGFP clone and vector were kindly provided by Dr. J. Raingo (IMBICE, Argentina).

### Electrophysiology

The isolated cells were observed with a mechanically stabilized inverted microscope (Telaval 3, Carl Zeiss, Jena, Germany) equipped with a  $\times 40$  objective lens. The test solutions were applied through a multibarreled pipette positioned close to the target cell. After each experiment on a single cell, the experimental chamber was replaced by another one containing a new sample of cells. All experiments were performed at room temperature ( $\sim 22^\circ\text{C}$ ).

The standard tight-seal inside-out and whole-cell configurations of the patch-clamp technique [19] were used to record single-channel and macroscopic currents. Glass pipettes were drawn from WPI PG52165-4 glass on a two-stage vertical micropipette puller (PP-83, Narishige Scientific Instrument Laboratories, Tokyo, Japan) and pipette resistance ranged from 2 to 4 M $\Omega$ .

### Single-channel recordings in HUASMCs

Single-channel currents were recorded in the inside-out configuration (IO), filtered with a four-pole lowpass Bessel filter at 2 kHz (Axopatch 200A amplifier, Axon Instruments, Foster City, CA) and digitized (Digidata 1200 Axon Instruments, Foster City, CA) at 16 kHz. Voltage-clamp recordings were taken up to 30–60 s at different membrane potentials to obtain the single channel current amplitude, the open probability (NPo), and the mean open and closed dwell times of the channels. The identification of BK<sub>Ca</sub> channel presence in the patch was based on its unitary conductance value, voltage-dependent activity, and activation by an increase in intracellular Ca<sup>2+</sup> concentration, as we described before [31]. The control pipette solution used for single-channel recordings contained the following (in millimolars)—140 KCl, 0.5 MgCl<sub>2</sub>, 10 HEPES, 6 glucose, 1 CaCl<sub>2</sub>, 5 4-aminopyridine (4-AP), pH adjusted to 7.4 with HCl. 4-AP was added to block K<sub>v</sub> channels present in HUASMCs [33]. The bath solution (BS) in contact with the cytosolic face of the membrane contained the following (in millimolars)—140 KCl, 0.5 MgCl<sub>2</sub>, 10 HEPES, 6 glucose, 1 EGTA, pH adjusted to 7.4 with KOH. Different amounts of CaCl<sub>2</sub> were added to the BS so as to establish the desired free Ca<sup>2+</sup> concentrations, according to the BK<sub>Ca</sub> channel activity needed for each protocol (100, 50, or 3 nM; calculated using Maxchelator software from Stanford University: <http://maxchelator.stanford.edu>).

The effects of lithocholic acid (LT) and AA on BK<sub>Ca</sub> channels were tested by adding the adequate quantity to the BS so as to reach a final concentration of 150 and 10  $\mu\text{M}$ , respectively.

Single-channel currents were analyzed with Clampfit software (Molecular Devices, version 10.3). Open probability, as well as closed and open dwell times were studied in steady state conditions. Open probability is expressed as NPo below, where  $N$  is the number of single channels present in each patch, and its values were calculated using the following expression:

$$NPo = \frac{\sum_{j=1}^n jt_j}{T}$$

where  $T$  is the recording duration and  $t_j$  is the time spent with  $j=1,2,3,\dots,n$  channels open. Stationary conditions of single channel recordings were controlled by plotting the NPo values calculated for intervals of 5 s of recording as time function (stability plot). The effect of AA on BK<sub>Ca</sub> channel open and closed dwell times was tested only in patches containing a single BK<sub>Ca</sub> channel. Stability plots were also obtained in order to confirm stationary values in both conditions. They were constructed to represent the time spent in the closed (or open) state for every channel closure (or aperture) plotted as a function of recording time. NPo and dwell time values in the presence and absence of AA were obtained from single channel event detection by the half-amplitude threshold criterion. The mean values of these parameters, in control conditions and after AA perfusion, were calculated when these reached stable values.

A voltage ramp protocol was used to measure the effect of AA on BK<sub>Ca</sub> single channel open probability at different voltages. This method was based on that described by Carl and Sanders [10], in which multiple voltage ramps are applied to an IO patch in order to obtain a single channel average current ( $\bar{i}$ ) versus voltage (volts) relationship ( $\bar{i}$ -V curve). Considering that, at a given potential,  $\bar{i}$  is equal to NPo $\times i$  (where  $i$  is the channel current amplitude at this potential), Po vs voltage relationship (Po-V curve) can be obtained by dividing the  $\bar{i}$ -V curve by the N $\times i$  values at each potential. Before testing AA effects, we adapted this protocol to HUASMC BK<sub>Ca</sub> channels. First, we tested different intracellular Ca<sup>2+</sup> concentrations (100, 50, and 3 nM) in order to establish adequate channel basal activity (data not shown). Then, we tested both depolarizing and hyperpolarizing voltage ramp protocols at different rates of applied potential change (0.02, 0.04, 0.08, or 0.16 mV/ms) so as to select a protocol that would be slow enough to avoid Po-V distortion by the time constants of voltage-dependent channel activation or deactivation phenomena (data not shown). With the information provided by these experiments, we constructed a voltage protocol consisting of a 500 ms voltage step from a

holding potential of  $-80$  mV to  $+80$  mV (to obtain steady-state activation) followed by a  $0.08$  mV/ms hyperpolarizing voltage ramp to  $-80$  mV. This protocol was applied between 15 and 75 times in a BS with  $50$  nM free  $\text{Ca}^{2+}$  concentration, both before and after AA perfusion. After that,  $\bar{v}$ -V and Po-V curves were constructed. Finally, the Po-Vs were fitted using the GraphPad Prism (version 5.03) with a Boltzmann relationship assuming a  $\text{Po}_{\text{max}}$  of 1, since the membrane patches was disrupted in extremely depolarized steps, where maximal Po could be observed. The equation used to fit these curves was:

$$Po = \frac{1}{1 + e^{-\frac{zF(V_{1/2} - V)}{RT}}}$$

where  $V_{1/2}$  is the potential at which Po is 0.5,  $z$  is a constant value that describes voltage sensibility (steepness of the curve),  $F$  is the Faraday constant ( $96,500$  C/mol),  $R$  is the gas constant ( $8.314$  J/(mol $\times$ K)), and  $T$  is room temperature (approximately  $298$  K).

To study the effect of AA on  $\text{BK}_{\text{Ca}}$  channel voltage activation kinetics, we carried out a protocol to examine the latency to the first channel opening after a voltage depolarizing step. Since most patches recorded in HUASMCs contained more than a single  $\text{BK}_{\text{Ca}}$  channel, we proceeded as described by Aldrich et al. [2]. A  $500$  ms voltage step from a holding potential of  $-80$  to  $+80$  mV was applied on IO patches with less than four copies of  $\text{BK}_{\text{Ca}}$  channels, and this was repeated at least 50 times for each patch with and without  $10$   $\mu\text{M}$  AA. Latencies were then measured to represent the delay of the first channel openings after the voltage step. A cumulative histogram was then constructed with the latencies of such first openings measured in both conditions, thus resulting in the cumulative density function (cdf). The count was expressed in probabilities, and for patches containing more than a single channel, the true first latency distribution was obtained by taking the  $N^{\text{th}}$  root of the apparent distribution function, where  $N$  is the number of channels present in the patch [2]. Further on, the distributions were fitted with Clampfit software with the following first-order exponential decay function:

$$\text{cdf} = Ae^{-t/\tau_{\text{act}}}$$

where  $\tau_{\text{act}}$  is the time constant of voltage activation.

#### Whole-cell recordings in HUASMCs

Whole-cell currents were filtered with a four-pole lowpass Bessel filter (Axopatch 200A amplifier) at  $2$  kHz and digitized (Digidata 1200 Axon Instruments) at a sample frequency of  $20$  kHz. The experimental recordings were stored on a computer hard disk for later analysis. The pipette solution contained the following (in millimolars)— $130$  KCl,  $10$  HEPES,  $0.1$  EGTA,  $1$  MgCl<sub>2</sub>,  $0.1$  CaCl<sub>2</sub>,  $5$  ATP-Na<sub>2</sub>; pH was adjusted to  $7.4$  with KOH yielding a calculated free

$\text{Ca}^{2+}$  concentration of  $750$  nM. The BS contained the following (in millimolars)— $130$  NaCl,  $5.4$  KCl,  $1.2$  MgCl<sub>2</sub>,  $2.5$  CaCl<sub>2</sub>,  $5$  HEPES,  $6$  glucose, pH was adjusted to  $7.4$  with NaOH. In some experiments,  $5$  mM 4-AP or  $500$  nM paxilline were added to the BS in order to inhibit the  $\text{K}_{\text{V}}$  or  $\text{BK}_{\text{Ca}}$  channel contribution to the macroscopic current, respectively [31, 33]. Whole-cell current stability was monitored by applying successive  $500$  ms voltage steps (from a holding potential of  $-50$  mV to a test potential of  $+40$  mV), discarding cells in which the current amplitude did not remain constant in time. After the current was stable, the same voltage-clamp step protocol was applied in the control or in the presence of AA. After current stabilization, a voltage-clamp step protocol, which consisted in a family of  $500$  ms voltage steps between  $-70$  and  $+60$  mV from a holding potential of  $-50$  mV, was applied both in the control and in the presence of AA, for further current–voltage relationship (I-V) analysis. Cell membrane capacitance was calculated from the capacity current obtained from the recording of a single  $10$  mV hyperpolarizing step. With the aim to quantify the macroscopic kinetics of activation, a first-order exponential function was used to fit these recordings. The equation that was used to fit with the Clampfit software was:

$$I_x = Ae^{-t/\tau_x}$$

where  $\tau_x$  is the time constant of activation from the current evoked ( $I_x$ ) by a voltage pulse to  $x$  mV.

#### Inside-out macroscopic current recordings in heterologously expressed $\text{BK}_{\text{Ca}}$ channels

Macroscopic currents of  $\text{BK}_{\text{Ca}}$  channel expressed in HEK293T cells were recorded using the cell-free inside-out configuration. Currents were filtered with a four-pole lowpass Bessel filter (Axopatch 200A amplifier) at  $2$  kHz and digitized (Digidata 1200 Axon Instruments) at a sample frequency of  $20$  kHz. The experimental recordings were stored on a computer hard disk for later analysis. The pipette solution contained the following (in millimolars)— $140$  KCl,  $0.5$  MgCl<sub>2</sub>,  $10$  HEPES,  $6$  glucose,  $1$  CaCl<sub>2</sub>; pH was adjusted to  $7.4$  with KOH. The BS contained the following (in millimolars)— $140$  KCl,  $0.5$  MgCl<sub>2</sub>,  $10$  HEPES,  $6$  Glucose,  $1$  EGTA, pH adjusted to  $7.4$  with KOH yielding a calculated free  $\text{Ca}^{2+}$  concentration of  $3$  nM (calculated using MaxChelator software from Stanford University: <http://maxchelator.stanford.edu>). The effect of AA on  $\text{BK}_{\text{Ca}}$  channels was tested by adding the adequate quantity to the BS so as to reach a final concentration of  $10$   $\mu\text{M}$ . Current stability was monitored by applying successive  $150$  ms voltage steps (from a holding potential of  $0$  mV to a test potential of  $+120$  mV), discarding cells in which the current amplitude did not remain constant in time. The same voltage-clamp step protocol was applied in



control conditions as in presence of AA. After current stabilization, a voltage-clamp step protocol, which consisted in a family of 180 ms voltage steps between  $-50$  and  $190$  mV from a holding potential of  $0$  mV followed by a  $50$  ms voltage step to  $-50$  mV, was applied both in the control and in the presence of AA, for further conductance–voltage relationship (G-V) analysis. The G-V curves were fitted using the GraphPad Prism (version 5.03) with a Boltzmann relationship. The equation used to fit these curves was:

$$\frac{G}{G_{\max}} = \frac{1}{1 + e^{\frac{-zF(V_{1/2} - V)}{RT}}}$$

where  $V_{1/2}$  is the potential at which  $\frac{G}{G_{\max}}$  is 0.5,  $z$  is a constant value that describes voltage sensibility (steepness of the curve),  $F$  is the Faraday constant ( $96,500$  C/mol),  $R$  is the gas constant ( $8.314$  J/(mol $\times$ K)), and  $T$  is room temperature (approximately  $298$  K).

#### Drugs and reagents used

AA, LT, paxilline, 4-AP, EGTA,  $\text{Na}_2\text{ATP}$ , and collagenase used for cell isolation were purchased from Sigma Chemical Co. All other reagents were of analytical grade and purchased from local suppliers as well as DMEM medium and FBS. AA, LT, and paxilline were dissolved in dimethyl sulfoxide (DMSO). Fresh aliquots of stock solutions of AA, LT, and paxilline were added to the bath solution on the day of the experiment. An appropriate amount of DMSO was added to all control solutions without AA, LT, and paxilline. AA stock solution was stored at  $-20^\circ\text{C}$  in an  $\text{N}_2$ -atmosphere to prevent drug oxidation.

#### Statistics

The results are expressed as mean $\pm$ standard error of the mean. Paired or unpaired Student  $t$  tests were used to compare two groups. ANOVA test was used to compare three groups. For the comparison of frequency of instantaneous kinetics observed in whole cell currents before and after AA perfusion, the Chi-square test was used. In all cases, a  $P$  value lower than  $0.05$  was considered for establishing statistically significant differences.

## Results

Lithocholic acid (LT) effect on  $\text{BK}_{\text{Ca}}$  channels in human umbilical artery (HUA) smooth muscle cells (SMCs): a functional evidence for the presence of the  $\beta_1$ -accessory subunit

Bukiya et al. (2007–2011) have clearly demonstrated that LT activates  $\text{BK}_{\text{Ca}}$  channels only in the presence of accessory  $\beta_1$ -

subunits [5, 7]. This effect is mediated by a direct interaction between the lithocholate and the steroid interaction site in transmembrane domain 2 of the  $\beta_1$ -subunit [6]. Considering that the  $\text{BK}_{\text{Ca}}$  channel is commonly associated with  $\beta_1$ -subunits in native VSMCs [24, 25], we tested the effect of  $150$   $\mu\text{M}$  LT on  $\text{BK}_{\text{Ca}}$  channel activity in freshly isolated HUASMCs, so as to confirm the presence of this accessory subunit in these cells. The effects of LT on  $\text{BK}_{\text{Ca}}$  channels were studied at the single channel level in the IO configuration under symmetrical  $\text{K}^+$  concentration, which is an experimental condition where we have largely characterized  $\text{BK}_{\text{Ca}}$  channels in these cells [31]. Figure 1 presents a typical recording and mean NPo values showing a significant  $\text{BK}_{\text{Ca}}$  channel activation induced by LT, indicating that  $\text{BK}_{\text{Ca}}$  channel  $\alpha$  subunits are likely to be associated with accessory  $\beta_1$ -subunits in this cell type. Since LT activation occurs in all copies ( $n=1-3$ ) of  $\text{BK}_{\text{Ca}}$  channels present in all patches ( $n=7$ ) tested, the probability of finding a channel formed by  $\alpha$ -alone,  $\alpha$ - $\beta_2$ ,  $\alpha$ - $\beta_3$ , or  $\alpha$ - $\beta_4$  subunits was negligible. Therefore, the AA effects described below on  $\text{BK}_{\text{Ca}}$  channel activity and kinetics corresponds to this  $\alpha$ - $\beta_1$  association.

Arachidonic acid (AA) increases single channel  $\text{BK}_{\text{Ca}}$  activity in SMCs freshly isolated from HUA

The effects of AA on  $\text{BK}_{\text{Ca}}$  channels were studied at the single channel level in the IO configuration in the same conditions described before [31]. First, the effect of  $10$   $\mu\text{M}$  AA was tested on steady-state channel activity at  $+40$  mV membrane potential. AA produces a reversible increase in  $\text{BK}_{\text{Ca}}$  channel open probability without modifying its conductance value. Figure 2 shows a typical recording of channel activation and after 4 min washout (Fig. 2a), followed by its stability plot (Fig. 2b), where the open probability (expressed as NPo) was calculated every 5 s and plotted as a function of the recording time. It is possible to observe that AA slowly increases the NPo of the  $\text{BK}_{\text{Ca}}$  channel, reaching maximal steady-state activation after about 4–5 min of AA perfusion. AA induced a significant rise in NPo values from  $0.01113 \pm 0.00741$  under control conditions to  $0.10992 \pm 0.06129$  after stable AA effect; this activation was reversible after 4 min of AA washout where the NPo fell to  $0.00875 \pm 0.00417$ , returning to control values ( $P < 0.05$ ,  $n=6$  patches from three umbilical cord donors).

Kinetic analysis was performed by detecting single channel events based on the half-amplitude threshold criterion in all patches containing a single  $\text{BK}_{\text{Ca}}$  channel ( $n=4$ ). Stability plots of closed and open dwell times, both in control conditions and during AA perfusion, were constructed by plotting the time that the channel remained in every closed (or open) state event as a function of time recording (Fig. 2c and d, respectively). In accordance to the NPo analysis, these graphs show that open and closed dwell times of AA-induced  $\text{BK}_{\text{Ca}}$

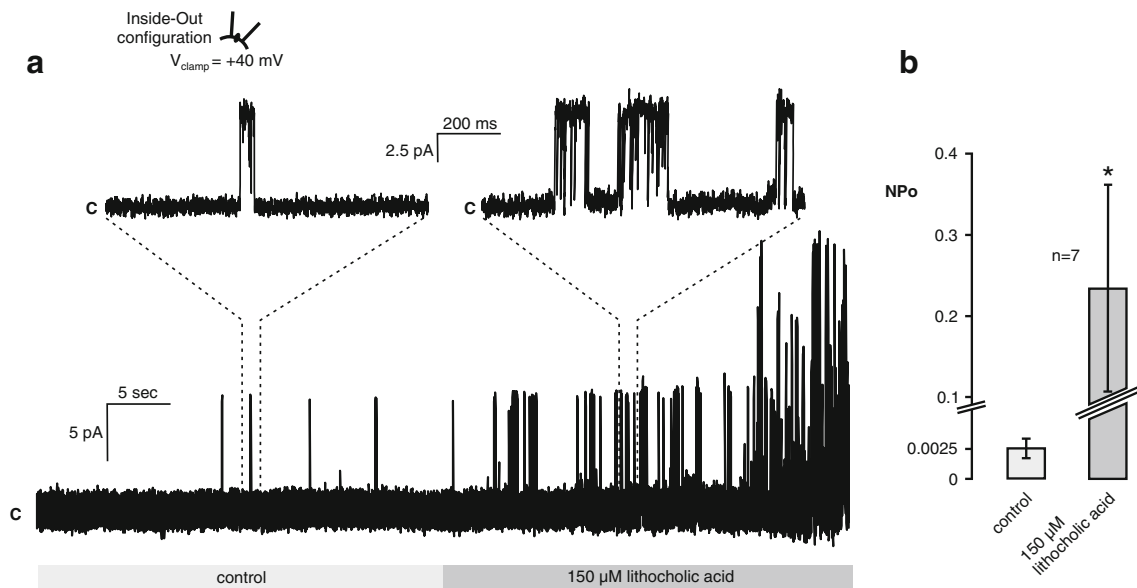


**Fig. 1** Lithocholic acid activates the high-conductance voltage- and  $\text{Ca}^{2+}$ -activated  $\text{K}^+$  channels ( $\text{BK}_{\text{Ca}}$ ) in human umbilical artery (HUA) smooth muscle cells (SMC) in the inside-out (IO) single-channel configuration **a** Typical recording of lithocholic acid ( $150 \mu\text{M}$ ) effect in an IO patch containing 2  $\text{BK}_{\text{Ca}}$  channel copies clamped at  $+40 \text{ mV}$ . The closed

level is indicated as **c**. **b** Mean activity values (NPo) of  $\text{BK}_{\text{Ca}}$  channels recorded as shown in **a** in control conditions and with  $150 \mu\text{M}$  lithocholic acid ( $n=7$  patches from six umbilical cord donors). The asterisk indicates statistically significant difference from controls (Student's *t* test,  $P<0.05$ )

channel activation reach a stable value after about 4 min of perfusion. The analysis of mean closed and open times before and after AA indicates that both significantly changed with AA. Specifically, there was a reduction of mean closed time from  $2,090.9 \pm 604.2 \text{ ms}$  to  $208.3 \pm 53.7 \text{ ms}$  and an increase in mean open time from  $7.8 \pm 0.3 \text{ ms}$  to  $13.2 \pm 1.3 \text{ ms}$  in tested cells ( $P<0.05$ ,  $n=4$  patches from three umbilical cord donors). These results indicate that the increase of NPo induced by AA is primarily caused by a tenfold decrease in the mean duration of closed dwell time.

Next, in order to study the voltage dependence of AA-induced  $\text{BK}_{\text{Ca}}$  channel activation, we performed a series of experiments using a voltage ramp protocol similar to that described by Carl and Sanders [10]. Working with  $50 \text{ nM}$  of  $\text{Ca}^{2+}$  in the solution in contact with the channel intracellular side, the patches were slowly hyperpolarized from  $+80$  to  $-80 \text{ mV}$  using a  $2 \text{ s}$  voltage ramp protocol. The rate of hyperpolarization ( $0.08 \text{ mV/ms}$ ) was slow enough to avoid data distortion by the deactivation time constant (see “Methods”, for more detail). This procedure was repeated between 15 and 75 times in each tested condition to obtain the mean current response. Typical superimposed recordings in the control condition and in the presence of  $10 \mu\text{M}$  AA are shown in Fig. 3a, and the corresponding mean current–voltage relationships ( $\bar{i}$ - $V$ ) drawn from the average currents are presented in Fig. 3b. The voltage-dependent activation of the  $\text{BK}_{\text{Ca}}$  channel can be best characterized by the relationship between Po and  $V$  (Po- $V$  curves). Accordingly, the mean  $\bar{i}$ - $V$  curves were transformed into a Po- $V$  curve by dividing each

data point of the averaged current by the number of copies of the channel in the patch and the single channel current amplitude at each potential. Figure 3c shows the mean Po- $V$  curves of the  $\text{BK}_{\text{Ca}}$  channel in the absence and presence of AA obtained from five patches. AA induced a shift in Po- $V$  curves to more hyperpolarized membrane potentials, achieving statistically significant difference in all voltages higher than  $+23 \text{ mV}$  ( $P<0.05$ ). It was not possible to observe maximal activation in Po- $V$  curves because more depolarized potentials, in general, disrupted the membrane patch. However, in order to quantify the shift effect of AA in Po- $V$  curves, we assumed  $\text{Po}_{\text{max}}$  as 1 and fitted these relationships by a Boltzmann function, thus observing that AA induces a significant  $20.13 \text{ mV}$  change in  $V_{1/2}$  (from  $124.7 \pm 1.5 \text{ mV}$  in control conditions to  $83.9 \pm 0.5 \text{ mV}$  in AA,  $P<0.05$ ) without significantly modifying the  $z$  value ( $1.407 \pm 0.060$  and  $1.286 \pm 0.034$  in control conditions and in AA respectively; NS,  $P=0.1178$ ).

Finally, we studied the effect of AA on  $\text{BK}_{\text{Ca}}$  channel voltage activation kinetics by analyzing the latency to the first channel opening. A  $500 \text{ ms}$  voltage step from a holding potential of  $-80$  to  $+80 \text{ mV}$  was applied in IO patches and repeated at least 50 times for each patch with and without  $10 \mu\text{M}$  AA. Representative single channel traces in both conditions are shown in Fig. 4a. It was observed that AA produces an increase of about a 20 % in the number of pulses with at least one single channel opening during voltage step (data not shown) and a reduction in the time delay to first channel opening (first latency).

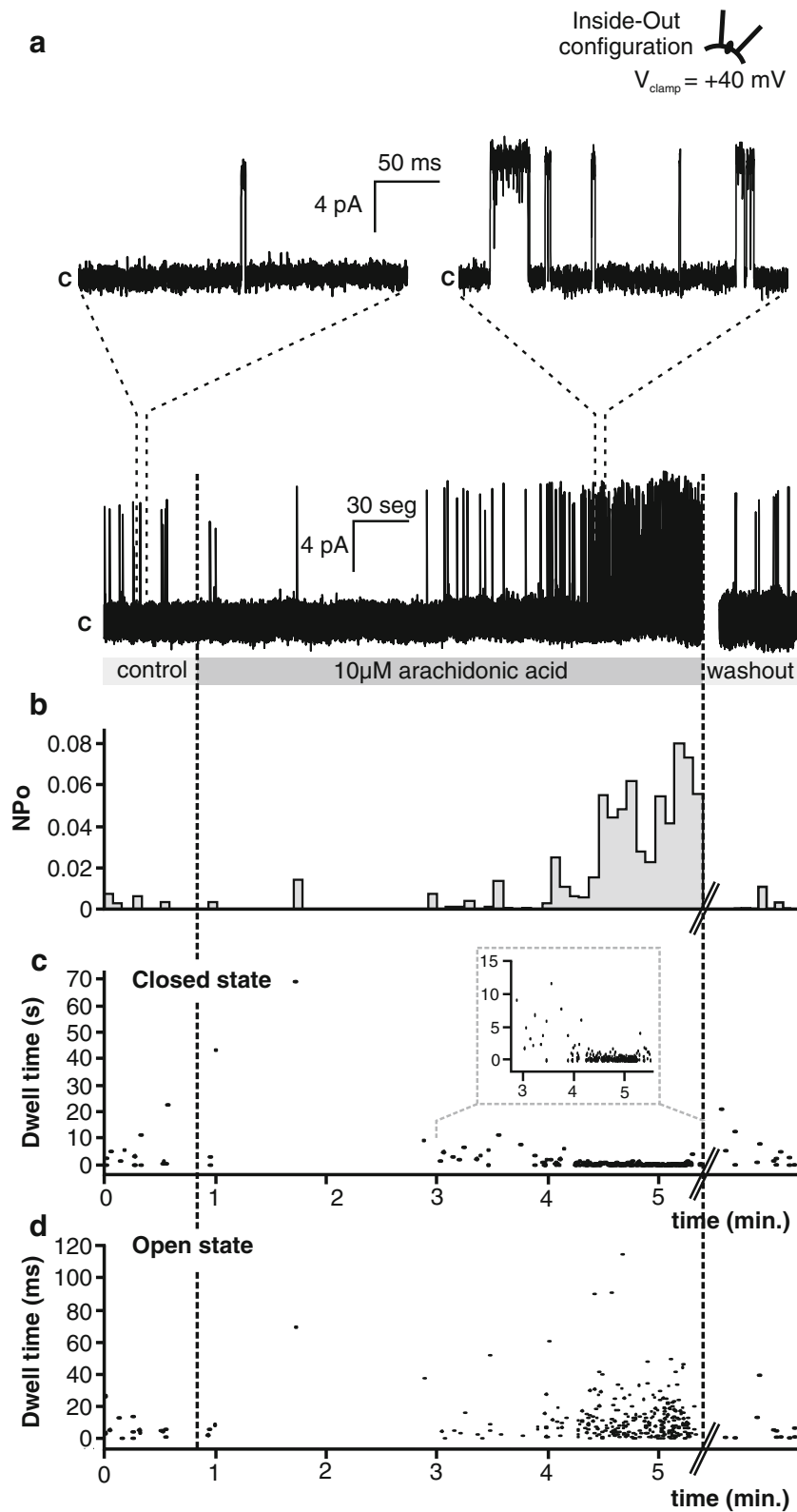


**Fig. 2** Time course of BK<sub>Ca</sub> channel activation produced by arachidonic acid (AA) in the IO configuration. **a** Representative traces of a single BK<sub>Ca</sub> channel in the HUASMC in an IO patch clamped at +40 mV in control condition, during 10  $\mu\text{M}$  AA perfusion and after 4 min of AA washout. The closed level is indicated as C. **b** Temporal course of the AA effect on BK<sub>Ca</sub> channel activity (NPo) obtained from channel recording shown in **a**. NPo

values were calculated every 5 s and plotted as function of recording time. **c**, **d** Dwell time stability plots of the BK<sub>Ca</sub> channel activation by AA obtained from channel recording shown in **a**. Each graph represents the time spent in closed (**c**) and open (**d**) state in every channel closure and aperture, respectively, plotted as function of recording time. The inset in **c** shows with high resolution the final portion of closed dwell time stability plot

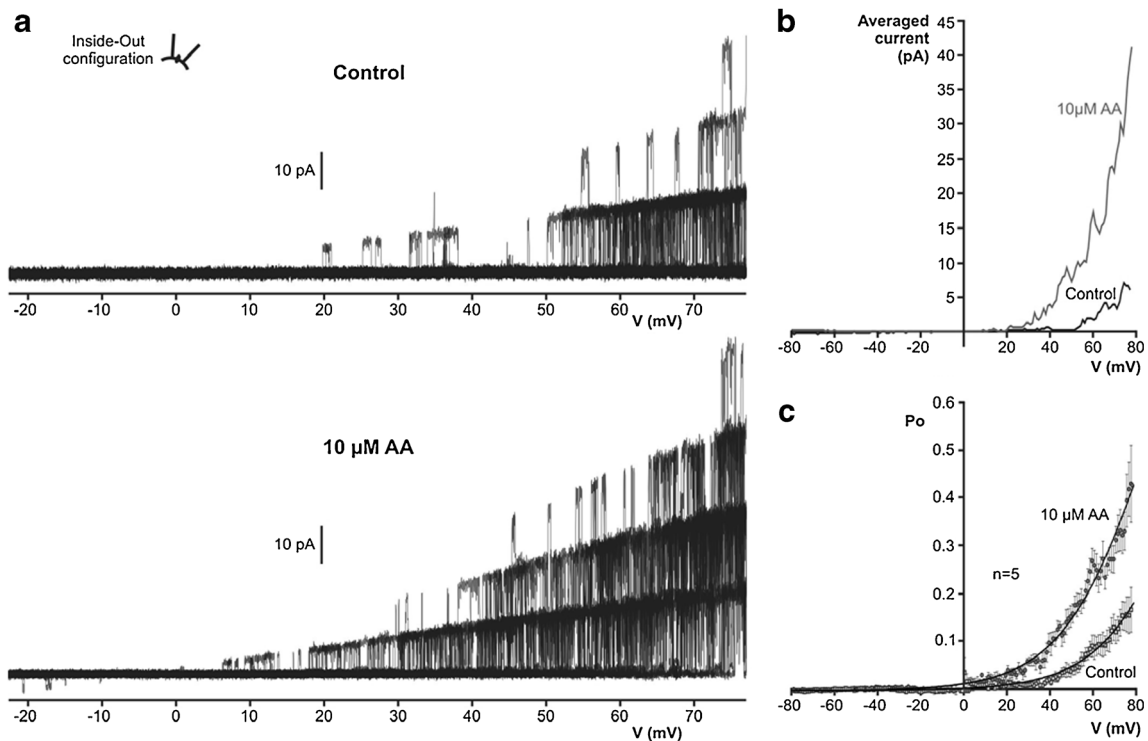


**Fig. 3** AA induces a shift to more hyperpolarized values in the voltage activation curve of BK<sub>Ca</sub> channel in HUA SMC in the IO configuration. **a** 30 superimposed representative recordings of BK<sub>Ca</sub> channels IO currents obtained by applying 80 mV/s hyperpolarizing voltage-ramp protocol from +80 to -80 mV (see “Methods”) in control conditions (*upper panel*) and after 10 μM AA perfusion (*lower panel*). The patch contains four channel copies. **b** Averaged current versus voltage curve obtained from recording shown in **a** in control conditions and with 10 μM AA. **c** Mean

voltage activation curves ( $P_o$  vs. voltage) of BK<sub>Ca</sub> channels in control conditions and with 10 μM AA ( $n=5$  patches from two umbilical cord donors).  $P_o$  was calculated from the averaged current, after correcting for the number of channels in the patch, the unitary conductance and the driving force (see “Methods”). Data points were fitted by a Boltzmann function (*solid lines*) taking  $P_o=1$  as maximal activation. Mean  $P_o$  values of BK<sub>Ca</sub> channel in AA showed statistically significant difference from controls in all voltages greater than +23 mV (Student’s *t* test,  $P<0.05$ )

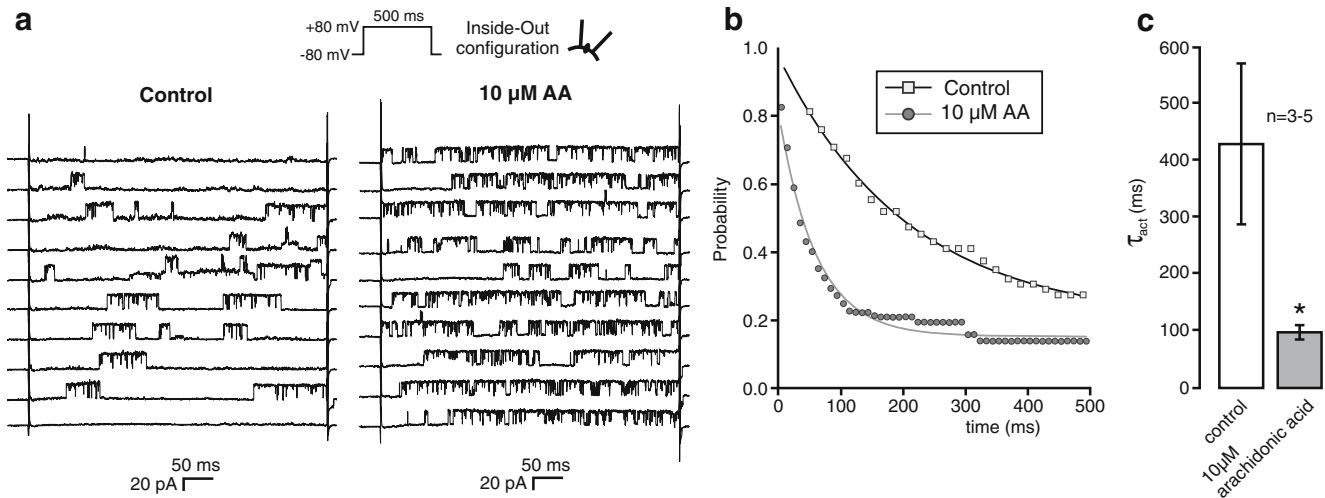


**Fig. 4** AA reduces the latency to the first channel open in depolarizing voltage step activation of BK<sub>Ca</sub> channel in HUA SMC in the IO configuration. **a** Ten representative recordings of BK<sub>Ca</sub> channels IO currents obtained by applying a potential step from -80 to +80 mV in control conditions and after 5 min of 10 μM AA perfusion. The patch contains a single BK<sub>Ca</sub> channel. **b** Cumulative distributions of first latencies corresponding to the same patch show in **a**, obtained after correcting for the number of channels in the patch (see “Methods”). These distributions

show the probabilities that the channel remained closed by the times indicated. Data points were fitted by a first-order exponential function (*solid lines*) in order to obtain the time constants of voltage activation ( $\tau_{act}$ ) in both conditions. **c** Mean time constants of voltage activation ( $\tau_{act}$ ) obtained as shown in **b** under control conditions and after 5 min of 10 μM AA perfusion ( $n=3-5$  patches from five umbilical cord donors). The *asterisk* indicates statistically significant difference from control (Student’s *t* test,  $P<0.05$ )



A cumulative histogram was then constructed with latencies to first openings measured in both conditions, so as to obtain the cumulative density function. For patches containing more than a single channel, the true first latency distribution was established by taking the  $N^{\text{th}}$  root of the apparent distribution function, where  $N$  is the number of channels present in the patch [2] (see “Methods”, for more details). These distributions show the probability that the channel still remains closed at the times indicated. As is shown in Fig. 4b, AA induced a shift to shorter first latencies in the cumulative distributions obtained from the recordings presented in Fig. 4a. The distributions from three to five different patches were fitted by a first-order exponential decay function, and the mean time constants of voltage activation  $\tau_{\text{act}}$  values were obtained for both conditions. The data presented in Fig. 4c shows that AA significantly decreases the  $\tau_{\text{act}}$  consistent with the acceleration of BK<sub>Ca</sub> channel voltage activation kinetics ( $P < 0.05$ ). These results are consistent with the ones obtained in the analysis of steady-state dwell times, since AA reduced the time that the channel remained closed in both cases, thus increasing the opening rate.

#### AA effects in whole-cell K<sup>+</sup> currents in HUASMCs

To analyze the effect of this FA on K<sup>+</sup> currents under a more physiological context, we tested the AA effect on macroscopic currents from HUASMCs. In a previous report, we demonstrated that the macroscopic voltage-dependent K<sup>+</sup> current in HUASMCs is mostly carried through two different types of ion channels: BK<sub>Ca</sub> channels and the voltage-dependent K<sup>+</sup> channels (K<sub>V</sub>) [33]. We also observed that this macroscopic current is completely inhibited when using 500 nM paxilline (a BK<sub>Ca</sub> channel blocker) and 5 mM 4-AP (a classical K<sub>V</sub> channels blocker) [31]. Consequently, to investigate AA effects on both components of macroscopic currents, we tested the effect of 10 μM AA on a family of currents evoked by 500 ms voltage steps between -70 and +60 mV from a holding potential of -50 mV in the presence of 5 mM 4-AP (Fig. 5) or 500 nM paxilline (Fig. 6). In agreement with single channel results, extracellular perfusion of 10 μM AA (in the presence of 5 mM 4-AP) significantly increased the amplitude of the outward whole-cell current. Mean current–voltage relationships (I–V curves, Fig. 5b) showed that current increments are statistically significant at membrane potential values between -30 and +50 mV. These results suggest that the AA-activated macroscopic current was mediated by BK<sub>Ca</sub> channels, so we confirmed them by testing the AA effect in the presence of 500 nM paxilline (without 4-AP). In such conditions AA had no effect, hence indicating that this FA is able to activate BK<sub>Ca</sub> channels as we observed at the single channel level, and it did not affect K<sub>V</sub> channel activity (Fig. 6).

As it is possible to see in Fig. 5b, the AA effect produces a left shift in the I–V curve, inducing significant cell membrane

hyperpolarization. The effect of AA on resting cell membrane potentials was evaluated by measuring the reversal potential ( $E_{\text{rev}}$ ) of the I–V relationships, where 10 μM AA changed this value by about 25 mV with respect to the control condition (Fig. 5c,  $P < 0.05$ ).

Consistent with the results obtained at the single channel level, AA induces a significant increase in activation kinetics of the voltage-induced whole-cell current. Time constants of activation ( $\tau_{\text{act}}$ ) were obtained by fitting the beginning of the whole-cell current at all membrane potentials, where possible, with a single exponential function. In Fig. 5d, the mean  $\tau_{\text{act}}$  values before and after 3 min of AA perfusion were plotted versus membrane potential. AA accelerated activation kinetics at all membrane potentials analyzed. Moreover, after 5 min of AA perfusion, the current kinetics changed from a time-dependent activation without inactivation to an instantaneous activation with a tight inactivation at most depolarized steps in 9 out of 11 tested cells (Fig. 5a) (chi square test,  $P < 0.05$ ).

#### Effect of the modulatory β<sub>1</sub>-subunit on AA activation of BK<sub>Ca</sub> channels expressed in HEK cells

In order to study the relevance of β<sub>1</sub>-subunit presence on AA BK<sub>Ca</sub> channel activation, we expressed the channel α-subunit in HEK293T cells with or without the β<sub>1</sub>-subunit and tested the AA effect on them. Figure 7 shows typical traces of macroscopic BK<sub>Ca</sub> channels currents recorded in cell-free inside-out configuration before and after AA perfusion. The AA had no effect on BK<sub>Ca</sub> expressed without the β<sub>1</sub>-subunit in all tested patches ( $n = 3$ ) but clearly activated the channel in presence of the modulatory β<sub>1</sub>-subunit (Fig. 7a and b, respectively). When G–V curves were constructed and fitted with a Boltzmann equation, we observed that the activation of α–β<sub>1</sub> complex is characterized by a significant left shift on G–V curves without modification of apparent voltage sensitivity in accordance with results observed in native HUASMCs (Fig. 7c). The  $V_{1/2}$  was changed from 141.3 ± 2.0 mV under control conditions to 86.1 ± 3.9 mV in presence of AA ( $P < 0.0001$ ), while the  $z$  value was unaffected by AA (1.047 ± 0.085 and 1.098 ± 0.156 in control conditions and in AA, respectively; NS,  $P = 0.7755$ ). These results suggest that presence of the auxiliary β<sub>1</sub>-subunit is necessary to mediate the AA effect on BK<sub>Ca</sub> channel described above.

## Discussion

The present study demonstrates that AA, an endogenous PUFA, directly activates BK<sub>Ca</sub> channels present in HUASMCs. Moreover, taking into account that LT is able to activate BK<sub>Ca</sub> channels only if they are associated to β<sub>1</sub>-subunits [5, 7], BK<sub>Ca</sub> channel activation by LT (showed in Fig. 1) denotes functional evidence of such association.

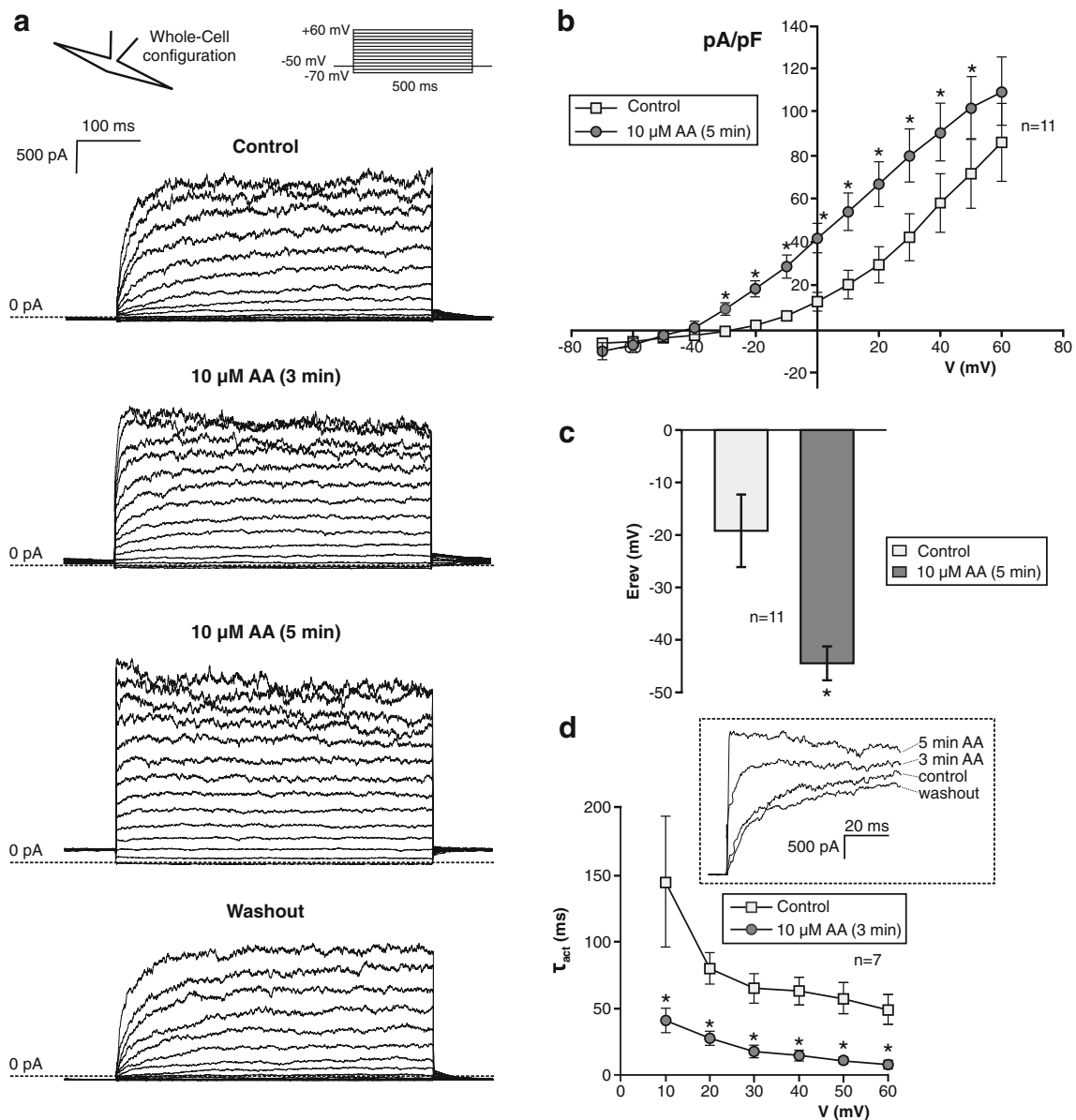


**Fig. 5** AA increases the BK<sub>Ca</sub> channel component of whole-cell (WC) K<sup>+</sup> currents in HUA SMC (recorded in 5 mM 4-aminopyridine) and accelerates its voltage activation kinetic. **a** Superimposed representative recordings of WC currents obtained by applying 10 mV voltage steps from  $-70$  to  $+60$  mV from a holding potential of  $-50$  mV in control conditions (first panel), after 3 and 5 min of  $10 \mu\text{M}$  AA perfusion (second and third panel, respectively) and after AA washout (fourth panel). **b** Mean current versus voltage (I-V) curves corresponding to the control conditions and 5 min of  $10 \mu\text{M}$  AA perfusion obtained in the same conditions as in **a** ( $n=11$  cells from two umbilical cord donors). **c** Mean  $E_{\text{reversal}}$  values corresponding to the control conditions and 5 min of  $10 \mu\text{M}$  AA perfusion obtained from the I-V curves recorded in the same

Together, our results provide the first evidence that AA is able to activate BK<sub>Ca</sub> channels modulated by the  $\beta_1$ -subunit in human vascular smooth muscle cells. Additionally, the effect of AA on the BK<sub>Ca</sub> channel expressed with or without the  $\beta_1$ -subunit demonstrates the requirement of  $\beta_1$ -subunit modulation to obtain the channel activation by this fatty acid.

conditions as in **a** ( $n=11$  cells from two umbilical cord donors). **d** Mean time constants of activation ( $\tau_{\text{act}}$ ) obtained from a first-order exponential function fit of the recording traces evoked by a potential step from a holding of  $-50$  to  $+10$ – $60$  mV, corresponding to control conditions and after 3 min of  $10 \mu\text{M}$  AA perfusion ( $n=7$  cells from two umbilical cord donors). The inset in **d** shows with high resolution the typical recording traces evoked by a potential step from  $-50$  to  $+60$  mV in control conditions, after 3 and 5 min of  $10 \mu\text{M}$  AA perfusion and after AA washout. All experiments were made in presence of 5 mM 4-aminopyridine in order to inhibit K<sub>V</sub> channels. The asterisk indicates statistically significant difference from control (Student's *t* test,  $P<0.05$ )

The AA-induced BK<sub>Ca</sub> channel activation observed in the excised patch IO configuration (in HUASMCs and in HEK cells) indicates that this PUFA has a direct effect on such channel activity, without metabolic modification by the different pathways that could produce AA metabolites [36, 38, 42]. Direct activation of the native BK<sub>Ca</sub> in IO patches was already

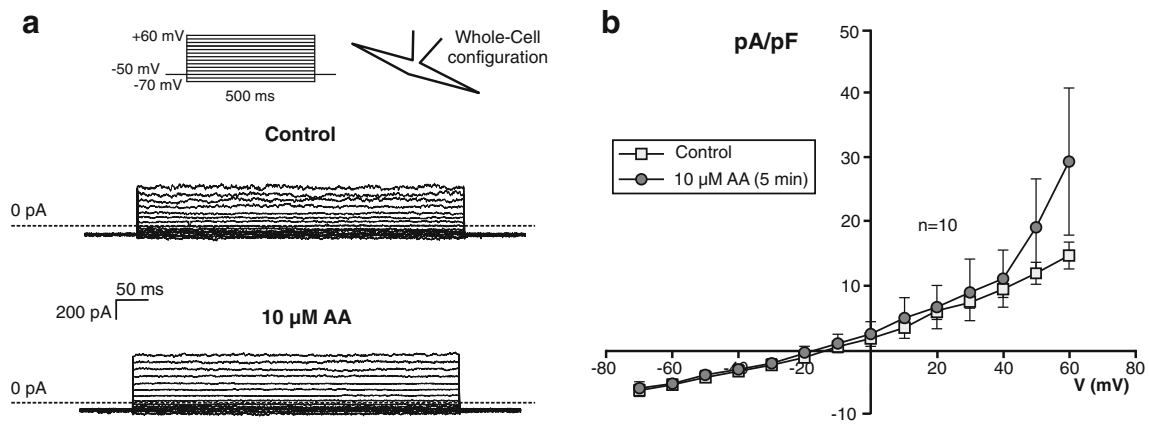


**Fig. 6** AA failed to activate the non-BK<sub>Ca</sub> channel component of WC K<sup>+</sup> currents in HUA SMC (recorded in 500 nM paxilline). **a** Superimposed representative recordings of WC currents obtained by applying 10 mV voltage steps from -70 to +60 mV from a holding potential of -50 mV in control conditions (*upper panel*) and after 5 min of 10 μM AA perfusion

(*bottom panel*) **b** Mean I-V curves corresponding to the control conditions and 5 min of 10 μM AA perfusion obtained in the same conditions as in **a** (n=10 cells from six umbilical cord donors). All experiments were made in presence of 500 nM paxilline in order to inhibit BK<sub>Ca</sub> channels. No statistically significant difference were observed (Student's *t* test, *P*<0.05)

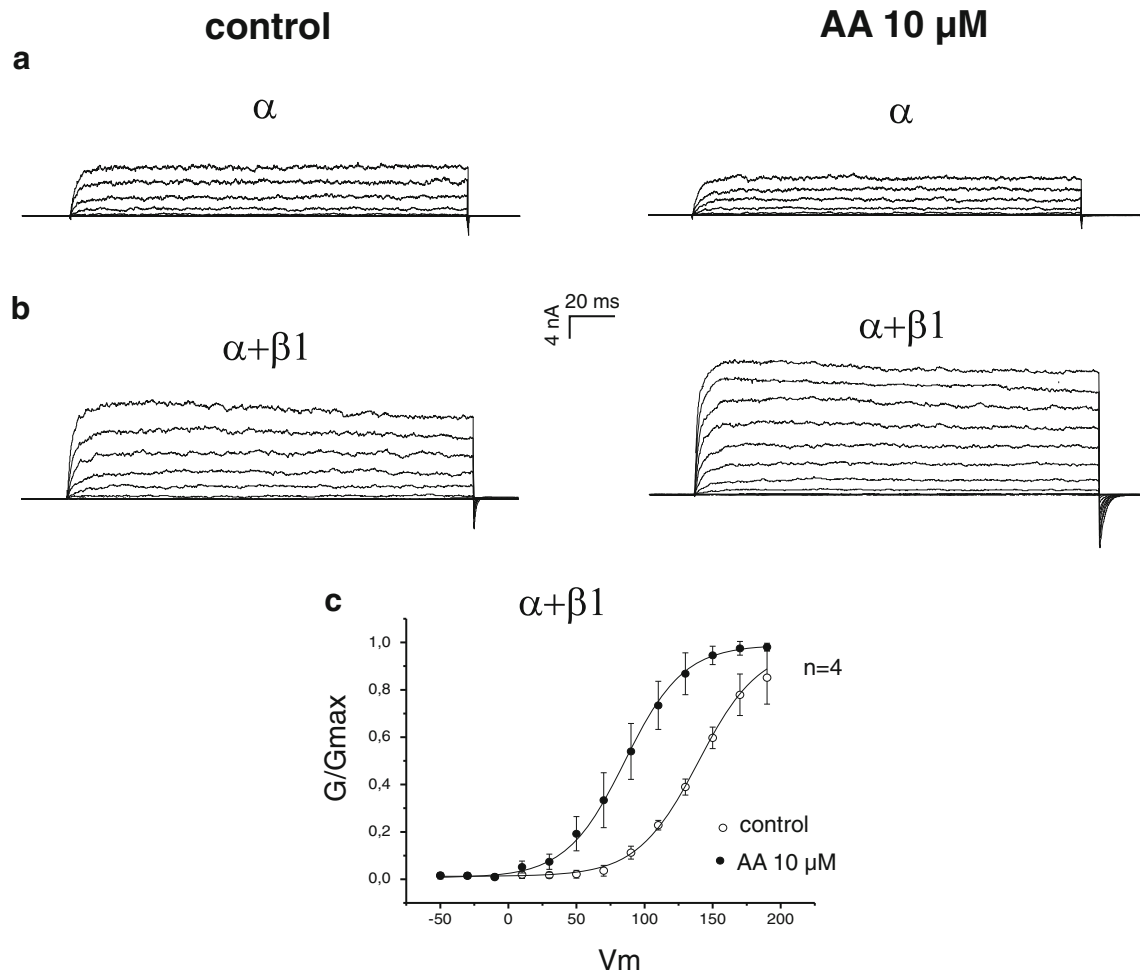


**Fig. 7** The presence of accessory β<sub>1</sub>-subunits is necessary for AA activation in BK<sub>Ca</sub> expressed in HEK cells. Superimposed representative IO currents of BK<sub>Ca</sub> channels, expressed in HEK cells with **(b)** or without the β<sub>1</sub>-subunit **(a)** before (*left*) and after 5 min of 10 μM AA perfusion (*right*). The currents were elicited in response to 20 mV voltage steps

from -70 to +190 mV from a holding potential of 0 mV. **c** Mean normalized conductance versus voltage (G-V) curves corresponding to the control conditions and 5 min of 10 μM AA perfusion obtained in BK<sub>Ca</sub> channel associated to β<sub>1</sub>-subunit (n=4 patches). Data points were fitted by a Boltzmann function (*solid lines*)

reported so as to discard the effect of AA by its metabolites in rabbit coronary [1] and pulmonary [11] SMCs, guinea pig gastric myocytes [46], and GH3 cells [12]. In the present study, our experiments performed at the single channel level allowed us to analyze in depth the mechanism of the stimulatory effect of AA on BK<sub>Ca</sub> channels present in HUASMCs.

When the voltage ramp protocol was applied on the IO configuration in HUASMCs, to study the effect of AA on BK<sub>Ca</sub> channel open probability at different membrane potentials, we observed that the fatty acid induces a left-shift in Po-V curves. This indicates that AA can activate the channel at more negative membrane potential values, where the channel is usually closed, without modifying the steepness of the curve. This result was also observed in I-V curves from HUASMCs macroscopic WC currents and in G-V curves from BK<sub>Ca</sub> channels co-expressed with  $\beta_1$ -subunit in HEK cells. Previously, Ahn et al. as well as Denson et al. observed a similar effect of AA on BK<sub>Ca</sub> channel Po-V curves from rabbit coronary SMCs and GH3 cells, respectively [1, 12]. The fact that AA induces this left shift on Po-V and G-V curves without modifying the slope in all cases suggests that the AA effect is not mediated by a modification of channel voltage sensitivity. However, up to now, the mechanism of AA-induced BK<sub>Ca</sub> channel activation can be said to be poorly understood.

Our single channel analysis showed that the increase in BK<sub>Ca</sub> channel activity is mainly due to a decrease in closed state dwell times and, in a minor way, to an increase in open state dwell times. Since there are no reports in the literature about AA effects on BK<sub>Ca</sub> single channel kinetics, these results are the first to indicate that AA can activate the BK<sub>Ca</sub> channels through a destabilization of its closed state to greatly facilitate channel opening and also by a stabilization of its open state to prolong their open time duration (Fig. 8b). A similar effect on closed state dwell times has been previously reported by Morin et al. for the AA-metabolite 20-HETE on BK<sub>Ca</sub> channels from human airway SMC [35].

The decrease in BK<sub>Ca</sub> channel closed state stability induced by AA also generates acceleration in the activation kinetics of voltage-induced currents in HUASMCs, where AA clearly reduces latency to first BK<sub>Ca</sub> channel opening (in the IO configuration) and diminishes the activation time constants (in both IO and WC configurations). This acceleration in activation rates induced by AA has also been previously observed in different types of K<sup>+</sup> channels: by Gavrilo-Ruch et al. in K<sub>v</sub>1.5, hEAG1 and hEAG2 [16] and by Ferroni et al. in TREK-2 channels [14].

Since the kinetic analysis performed in HUASMCs reflects that AA modifies the gating ring behavior by destabilization of closed channel conformation, it is possible to postulate that this effect could be independent of  $\beta$ -subunit presence. However, it is known that auxiliary  $\beta_1$ -subunit can interact with the channel  $\alpha$ -subunit affecting the gating ring as well as the voltage sensor domain [3, 27, 28]. Thus, another possible

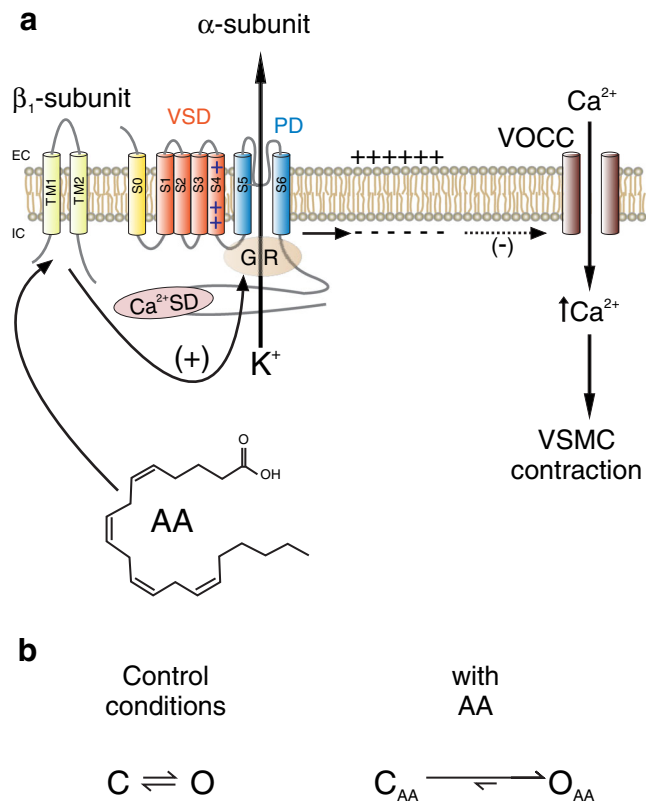


**Fig. 8** Summary of the action mechanism proposed to explain the AA-dependent activation of the BK<sub>Ca</sub> channel associated with the  $\beta_1$ -subunit in human VSMCs. **a** Arachidonic acid (AA) interacts with the  $\beta_1$ -subunit of BK<sub>Ca</sub> channel and modifies the operation of the gating ring. Moreover, the channel voltage sensitivity was unaffected by AA. Activator effect of AA induces a membrane hyperpolarization that can close VOCC (dotted black arrow) and lead to VSMC relaxation. PD pore domain, GR gating ring, VSD voltage sensor domain, Ca<sup>2+</sup>SD calcium sensor domain, VOCC voltage-operated calcium channel, VSMC vascular smooth muscle cell, EC extracellular side, IC intracellular side, TMI-2 transmembrane domain 1-2, S0-6 transmembrane segment 0-6. **b** Two states model can explain AA activator effect where AA binding to BK<sub>Ca</sub> channel destabilizes its close state and stabilizes its open state. C: close state, O: open state, C<sub>AA</sub>: AA-bonded close state, O<sub>AA</sub>: AA-bonded open state

mechanism to explain the AA effect on BK<sub>Ca</sub> channel is the interaction of the fatty acid with the ion channel by means of the auxiliary  $\beta_1$ -subunit. In order to confirm the relevance of  $\beta_1$ -subunit in AA BK<sub>Ca</sub> channel activation, we expressed the channel  $\alpha$ -subunit with or without the  $\beta_1$ -subunit in HEK cells, and we tested the effect of AA on them. Similarly to Sun et al. experiments [43], AA did not affect the BK<sub>Ca</sub> channel without any  $\beta$ -subunit expression, but accordingly with our HUASMCs results, in the presence of the  $\beta_1$ -subunit, the AA induces a significant channel activation (Fig. 7). Therefore, AA activation of BK<sub>Ca</sub> channels requires the presence of  $\beta_1$ -,  $\beta_2$ -, or  $\beta_3$ -subunits. However, our experimental results also suggest that the mechanism of AA activation of the  $\alpha$ - $\beta_1$  complex differs from the demonstrated by Sun et al. for the  $\alpha$ - $\beta_2$  complex where AA prevents the  $\beta_2$ -dependent channel inactivation.



Considering the experimental evidence presented in HUASMCs at single channel level and in BK<sub>Ca</sub> channels expressed in HEK, we are able to propose a more detailed action mechanism for AA activation of the BK<sub>Ca</sub> channel summarized in Fig. 8a. First, the AA acts by interacting with the  $\beta_1$ -subunit of BK<sub>Ca</sub> channel. Second, based on AA modification of BK<sub>Ca</sub> channel kinetics, this interaction is able to modify the operation of the gating ring (GR). Third, AA-BK<sub>Ca</sub> channel activation is independent of modification of the channel voltage sensitivity. Thus, the AA mainly produces, at the level of the BK<sub>Ca</sub> channel gating ring, a reduction on closed channel state stability, which increases the channel opening rate and the open probability (Fig. 8b).

Similar BK<sub>Ca</sub> channel activation in rat vascular SMCs by alteration of closed state stability, independent from voltage sensor activation and Ca<sup>2+</sup> binding, was recently reported by Hoshi et al. for DHA, a long-chain 22-carbon polyunsaturated omega-3 fatty acid [21]. Furthermore, they showed that the effect was enhanced by co-expression of  $\alpha$ -subunit with  $\beta_1$ - and  $\beta_4$ -subunits, compared with the  $\alpha$ -subunit alone or co-expressed with  $\beta_2$ - and  $\gamma$ -subunits [20]. By using mutagenesis, the authors proved that the TM1 N terminus domain from the  $\beta_1$ -subunit is essential for the DHA effect, thus suggesting that a direct interaction between the S6 domain ( $\alpha$ -subunit) and the TM1 N terminus ( $\beta_1$ -subunit) may be able to destabilize the closed state and increase open probability. This resemblance in both AA and DHA effects on BK<sub>Ca</sub> channel activation by destabilization of the closed state could involve a common binding site. However, the differential roles of  $\beta$ -auxiliary subunits on PUFA channel activation reported by Sun et al. and Hoshi et al. suggest that a more complex interaction is involved [20, 43].

Finally, on WC configuration, a more physiological recording condition where the cell remains with its membrane resting potential, it was possible to observe that the activator effect of AA generates a hyperpolarization that can lead to smooth muscle relaxation (Fig. 8a). Since in this configuration the three metabolic pathways remain intact, the effect of AA could be mediated by its metabolites. However, the effect of this fatty acid on BK<sub>Ca</sub> channel in the IO configuration (in HUASMCs and expressed in HEK cells) suggest that AA itself can contribute, in part, to smooth muscle hyperpolarization. These results highlights the role of AA itself as a possible second messenger molecule that can regulate channel activity under physiological and pathological conditions, leading to vasodilation and lower blood pressure values. Moreover, this last effect could explain the benefits of dietary consumption of the omega-6 fatty acid to obtain a cardiovascular protective effect.

**Acknowledgments** The authors wish to thank Ms. Anabel Poch and the staff of the Instituto Central de Medicina for the collection of umbilical cords. This study was financially supported by grant PIP 0202 from the Consejo Nacional de Investigaciones Científicas y Técnicas

(CONICET), Argentina, and by FONDECYT Grants 1120802, Anillo ACT 1104 (to Carlos Gonzalez), and the Chile–Argentina exchange grant 2011-665 CH/11/12 (to Veronica Milesi and Carlos Gonzalez from the Centro Interdisciplinario de Neurociencia de Valparaíso (The Interdisciplinary Center for Neuroscience in Valparaíso), a Millennium Institute.

Dr. Jessica Raingo generously contributed to this work by providing HEK293T cells, eGFP, and vector. We are grateful to Dr. Alejandro Rebolledo for critical feedback on the manuscript and to Francina Agosti for her helpful assistance in cell culturing and transfection.

## References

- Ahn DS, Kim YB, Lee YH, Kang BS, Kang DH (1994) Fatty acids directly increase the activity of Ca(2+)-activated K+ channels in rabbit coronary smooth muscle cells. *Yonsei Med J* 35(1):10–24
- Aldrich RW, Corey DP, Stevens CF (1983) A reinterpretation of mammalian sodium channel gating based on single channel recording. *Nature* 306(5942):436–441
- Bao L, Cox DH (2005) Gating and ionic currents reveal how the BKCa channel's Ca2+ sensitivity is enhanced by its beta1 subunit. *J Gen Physiol* 126(4):393–412. doi:10.1085/jgp.200509346
- Bendahhou S, Cummins TR, Agnew WS (1997) Mechanism of modulation of the voltage-gated skeletal and cardiac muscle sodium channels by fatty acids. *Am J Physiol* 272(2 Pt 1):C592–C600
- Bukiya AN, Liu J, Toro L, Dopico AM (2007) Beta1 (KCNMB1) subunits mediate lithocholate activation of large-conductance Ca2+-activated K+ channels and dilation in small, resistance-size arteries. *Mol Pharmacol* 72(2):359–369. doi:10.1124/mol.107.034330
- Bukiya AN, Singh AK, Parrill AL, Dopico AM (2011) The steroid interaction site in transmembrane domain 2 of the large conductance, voltage- and calcium-gated potassium (BK) channel accessory beta1 subunit. *Proc Natl Acad Sci U S A* 108(50):20207–20212. doi:10.1073/pnas.1112901108
- Bukiya AN, Vaithianathan T, Toro L, Dopico AM (2009) Channel beta2-4 subunits fail to substitute for beta1 in sensitizing BK channels to lithocholate. *Biochem Biophys Res Commun* 390(3):995–1000. doi:10.1016/j.bbrc.2009.10.091
- Burtis CA, Ashwood ER, Bruns DE (2006) Tietz textbook of clinical chemistry and molecular diagnostics, 4th edn. Elsevier Saunders, St. Louis
- Campbell WB, Falck JR (2007) Arachidonic acid metabolites as endothelium-derived hyperpolarizing factors. *Hypertension* 49(3):590–596. doi:10.1161/01.HYP.0000255173.50317.fc
- Carl A, Sanders KM (1990) Measurement of single channel open probability with voltage ramps. *J Neurosci Methods* 33(2–3):157–163
- Clarke AL, Petrou S, Walsh JV Jr, Singer JJ (2002) Modulation of BK(Ca) channel activity by fatty acids: structural requirements and mechanism of action. *Am J Physiol Cell Physiol* 283(5):C1441–C1453. doi:10.1152/ajpcell.00035.2002
- Denson DD, Wang X, Worrell RT, Eaton DC (2000) Effects of fatty acids on BK channels in GH(3) cells. *Am J Physiol Cell Physiol* 279(4):C1211–C1219
- Feletou M, Vanhoutte PM (2009) EDHF: an update. *Clin Sci (Lond)* 117(4):139–155. doi:10.1042/CS20090096
- Ferroni S, Valente P, Caprini M, Nobile M, Schubert P, Rapisarda C (2003) Arachidonic acid activates an open rectifier potassium channel in cultured rat cortical astrocytes. *J Neurosci Res* 72(3):363–372. doi:10.1002/jnr.10580
- Fink M, Lesage F, Duprat F, Heurteaux C, Reyes R, Fosset M, Lazdunski M (1998) A neuronal two P domain K+ channel stimulated by arachidonic acid and polyunsaturated fatty acids. *EMBO J* 17(12):3297–3308. doi:10.1093/emboj/17.12.3297



16. Gavrilova-Ruch O, Schonherr R, Heinemann SH (2007) Activation of hEAG1 potassium channels by arachidonic acid. *Pflügers Arch* 453(6):891–903. doi:10.1007/s00424-006-0173-3
17. Gonzalez-Corrochano R, La Fuente J, Cuevas P, Fernandez A, Chen M, Saenz de Tejada I, Angulo J (2013) Ca<sup>2+</sup>-activated K<sup>+</sup> channel (KCa) stimulation improves relaxant capacity of PDE5 inhibitors in human penile arteries and recovers the reduced efficacy of PDE5 inhibition in diabetic erectile dysfunction. *Br J Pharmacol* 169(2):449–461. doi:10.1111/bph.12143
18. Gonzalez C, Baez-Nieto D, Valencia I, Oyarzun I, Rojas P, Naranjo D, Latorre R (2012) K(+) channels: function-structural overview. *Compr Physiol* 2(3):2087–2149. doi:10.1002/cphy.c110047
19. Hamill OP, Marty A, Neher E, Sakmann B, Sigworth FJ (1981) Improved patch-clamp techniques for high-resolution current recording from cells and cell-free membrane patches. *Pflügers Arch* 391(2):85–100
20. Hoshi T, Tian Y, Xu R, Heinemann SH, Hou S (2013) Mechanism of the modulation of BK potassium channel complexes with different auxiliary subunit compositions by the omega-3 fatty acid DHA. *Proc Natl Acad Sci U S A* 110(12):4822–4827. doi:10.1073/pnas.1222003110
21. Hoshi T, Wissuwa B, Tian Y, Tajima N, Xu R, Bauer M, Heinemann SH, Hou S (2013) Omega-3 fatty acids lower blood pressure by directly activating large-conductance Ca(2+)-dependent K(+) channels. *Proc Natl Acad Sci U S A* 110(12):4816–4821. doi:10.1073/pnas.1221997110
22. Katz AM, Messineo FC (1981) Lipid-membrane interactions and the pathogenesis of ischemic damage in the myocardium. *Circ Res* 48(1):1–16
23. Klockner U (1993) Intracellular calcium ions activate a low-conductance chloride channel in smooth-muscle cells isolated from human mesenteric artery. *Pflügers Arch* 424(3–4):231–237
24. Knaus HG, Folander K, Garcia-Calvo M, Garcia ML, Kaczorowski GJ, Smith M, Swanson R (1994) Primary sequence and immunological characterization of beta-subunit of high conductance Ca(2+)-activated K<sup>+</sup> channel from smooth muscle. *J Biol Chem* 269(25):17274–17278
25. Knaus HG, Garcia-Calvo M, Kaczorowski GJ, Garcia ML (1994) Subunit composition of the high conductance calcium-activated potassium channel from smooth muscle, a representative of the mSlo and slowpoke family of potassium channels. *J Biol Chem* 269(6):3921–3924
26. Latorre R, Brauchi S (2006) Large conductance Ca<sup>2+</sup>-activated K<sup>+</sup> (BK) channel: activation by Ca<sup>2+</sup> and voltage. *Biol Res* 39(3):385–401
27. Liu G, Niu X, Wu RS, Chudasama N, Yao Y, Jin X, Weinberg R, Zakharov SI, Motoike H, Marx SO, Karlin A (2010) Location of modulatory beta subunits in BK potassium channels. *J Gen Physiol* 135(5):449–459. doi:10.1085/jgp.201010417
28. Liu G, Zakharov SI, Yang L, Wu RS, Deng SX, Landry DW, Karlin A, Marx SO (2008) Locations of the beta1 transmembrane helices in the BK potassium channel. *Proc Natl Acad Sci U S A* 105(31):10727–10732. doi:10.1073/pnas.0805212105
29. Liu L, Rittenhouse AR (2003) Arachidonic acid mediates muscarinic inhibition and enhancement of N-type Ca<sup>2+</sup> current in sympathetic neurons. *Proc Natl Acad Sci U S A* 100(1):295–300. doi:10.1073/pnas.0136826100
30. Marijic J, Li Q, Song M, Nishimaru K, Stefani E, Toro L (2001) Decreased expression of voltage- and Ca(2+)-activated K(+) channels in coronary smooth muscle during aging. *Circ Res* 88(2):210–216
31. Martin P, Enrique N, Palomo AR, Rebolledo A, Milesi V (2012) Bupivacaine inhibits large conductance, voltage- and Ca<sup>2+</sup>-activated K<sup>+</sup> channels in human umbilical artery smooth muscle cells. *Channels (Austin)* 6(3):174–180. doi:10.4161/chan.20362
32. Meves H (2008) Arachidonic acid and ion channels: an update. *Br J Pharmacol* 155(1):4–16. doi:10.1038/bjp.2008.216
33. Milesi V, Raingo J, Rebolledo A, Grassi de Gende AO (2003) Potassium channels in human umbilical artery cells. *J Soc Gynecol Investig* 10(6):339–346
34. Moreno C, Macias A, Prieto A, De La Cruz A, Valenzuela C (2012) Polyunsaturated fatty acids modify the gating of kv channels. *Front Pharmacol* 3:163. doi:10.3389/fphar.2012.00163
35. Morin C, Sirois M, Echave V, Gomes MM, Rousseau E (2007) Functional effects of 20-HETE on human bronchi: hyperpolarization and relaxation due to BKCa channel activation. *Am J Physiol Lung Cell Mol Physiol* 293(4):L1037–L1044. doi:10.1152/ajplung.00145.2007
36. Munaron L (2011) Shuffling the cards in signal transduction: calcium, arachidonic acid and mechanosensitivity. *World J Biol Chem* 2(4):59–66. doi:10.4331/wjbc.v2.i4.59
37. Nelson MT, Quayle JM (1995) Physiological roles and properties of potassium channels in arterial smooth muscle. *Am J Physiol* 268(4 Pt 1):C799–C822
38. Qiu Y, Quilley J (1999) Vascular effects of arachidonic acid in the rat perfused heart. Role of the endothelium, cyclooxygenase, cytochrome P450, and K(+) channels. *J Lipid Res* 40(12):2177–2184
39. Radenkovic M, Grbovic L, Radunovic N, Momcilov P (2007) Pharmacological evaluation of bradykinin effect on human umbilical artery in normal, hypertensive and diabetic pregnancy. *Pharmacol Rep* 59(1):64–73
40. Raingo J, Rebolledo A, Iveli F, Grassi de Gende AO, Milesi V (2004) Non-selective cationic channels (NSCC) in smooth muscle cells from human umbilical arteries. *Placenta* 25(8–9):723–729. doi:10.1016/j.placenta.2004.01.028
41. Shouk TA, Omar MN, Fayed ST (1999) Essential fatty acids profile and lipid peroxides in severe pre-eclampsia. *Ann Clin Biochem* 36(Pt 1):62–65
42. Smyth EM, Burke A, FitzGerald GA (2006) Lipid-derived autacoids: eicosanoids and platelet-activating factor. In: Brunton LL (ed) Goodman and Gilman's the pharmacological basis of therapeutics, 11th edn. Mc Graw-Hill, New York, pp 653–670
43. Sun X, Zhou D, Zhang P, Moczydlowski EG, Haddad GG (2007) Beta-subunit-dependent modulation of hSlo BK current by arachidonic acid. *J Neurophysiol* 97(1):62–69. doi:10.1152/jn.00700.2006
44. Sweet TB, Cox DH (2009) Measuring the influence of the BKCa {beta}1 subunit on Ca<sup>2+</sup> binding to the BKCa channel. *J Gen Physiol* 133(2):139–150. doi:10.1085/jgp.200810129
45. Yang Y, Li PY, Cheng J, Mao L, Wen J, Tan XQ, Liu ZF, Zeng XR (2013) Function of BKCa channels is reduced in human vascular smooth muscle cells from Han Chinese patients with hypertension. *Hypertension* 61(2):519–525. doi:10.1161/HYPERTENSIONAHA.111.00211
46. Zheng HF, Li XL, Jin ZY, Sun JB, Li ZL, Xu WX (2005) Effects of unsaturated fatty acids on calcium-activated potassium current in gastric myocytes of guinea pigs. *World J Gastroenterol* 11(5):672–675